

# Effect of the Alkyl Chain Length of the Cation on the Interactions between Water and Ammonium-Based Ionic Liquids: Experimental and COSMO-RS Studies

Varadhi Govinda,<sup>†</sup> T. Vasantha,<sup>†</sup> Imran Khan,<sup>‡</sup> and Pannuru Venkatesu<sup>\*,†</sup>

<sup>†</sup>Department of Chemistry, University of Delhi, Delhi 110 00 7, India

<sup>‡</sup>CICECO, Aveiro Institute of Materials, Chemistry Department, University of Aveiro, 3810-193 Aveiro, Portugal

## S Supporting Information

**ABSTRACT:** To improve the understanding of the molecular interactions of water with tetraalkyl ammonium-based ionic liquids (ILs) such as tetramethylammonium hydroxide, tetraethylammonium hydroxide, tetrapropylammonium hydroxide, and tetrabutylammonium hydroxide, thermophysical properties such as density ( $\rho$ ), speed of sound ( $u$ ), viscosity ( $\eta$ ) and refractive index ( $n_D$ ) were measured and a computational study using COSMO-RS was performed. The derived properties such as excess volumes ( $V^E$ ), deviation in isentropic compressibilities ( $\Delta\kappa_s$ ), deviation in viscosities ( $\Delta\eta$ ), and deviation in refractive indices ( $\Delta n_D$ ) under the same experimental conditions for these systems were also estimated. The observed  $V^E$  and  $\Delta\kappa_s$  values are negative over the entire composition of ILs at all investigated temperatures, whereas  $\Delta\eta$  and  $\Delta n_D$  values are positive under the same experimental conditions. These results reveal that the ammonium-based ILs significantly affect the intermolecular interactions between the solvent molecules. The computational study allows a qualitative analysis of the results in terms of the ion–dipole interactions, ion-pair formation, and hydrogen bonding between ammonium-based ILs and water.

## 1. INTRODUCTION

The framework of thermophysical properties of ionic liquids (ILs) and their mixtures with water is quite interesting and important for the chemical industry as well as various scientific fields.<sup>1–4</sup> For the past 15 years, the importance of ILs has been increasing because of their low volatility, nonflammability, high potential for recycling, and solvating properties for diverse substances.<sup>5–8</sup> Meanwhile, ILs became popular as “green solvents” with a wide range of potential applications such as removal of pollutants (H<sub>2</sub>S, CO<sub>2</sub>, and heavier hydrocarbons) and metal separation.<sup>9–13</sup> To understand the nature of ILs and their applications, knowledge of their thermophysical properties is essentially needed. The thermophysical properties, such as density ( $\rho$ ), ultrasonic sound velocity ( $u$ ), viscosity ( $\eta$ ), and refractive index ( $n_D$ ), of ILs and molecular solvent mixtures at various temperatures are of great fundamental and practical importance. Although the applications of ammonium-based ILs are increasing,<sup>14–19</sup> there remains a lack of data on the thermophysical properties of these ammonium-based ILs with water.

Water is one of the most abundant and greenest solvent; it has crucial and significant importance in both chemical and biochemical processes. From the studies reported to date on the interactions between ILs and water it seems that water mainly binds to the anion, but the interaction also depends on the cation.<sup>20–23</sup> The presence of water can dramatically affect the physical properties of ILs, such as their polarity, viscosity, and conductivity, even at low concentrations.<sup>24</sup> As a consequence, absorbed water may alter rates of chemical reactions and efficiencies of various processes in ILs. Even small amounts of water have shown significant effect in membrane applications,<sup>25</sup> cellulose processing,<sup>26</sup> and capturing CO<sub>2</sub>.<sup>27</sup>

Studies of binary mixtures of water and ILs have been increasing because of their application in absorption cooling,<sup>28–31</sup> distillation,<sup>29,32</sup> and extraction and purification of biomolecules and other value-added compounds.<sup>33–35</sup>

Although some fluorinated ILs are poorly soluble in water, even in these cases the water is highly soluble in the IL. The dissolution of water in the IL induces a major effect on their physicochemical properties.<sup>36,37</sup> The detailed knowledge of the thermophysical properties of ILs with water is essential for clarifying the molecular interactions between water and the ions of ILs. During the past years, a variety of the experimental data of thermophysical properties of imidazolium<sup>38–51</sup> pyridinium<sup>52–55</sup> pyrrolidinium<sup>56–60</sup> phosphonium<sup>61,62</sup> and ammonium<sup>34,63–68</sup> based ILs and water have been studied by various researchers. Among them, ammonium-based ILs, a subset of protic ILs, have shown potential as promising solvents in many scientific studies.<sup>69–72</sup>

Although the number of works on water and different ILs is increasing, there is still a lack of data regarding thermophysical properties of ammonium-based ILs with water.<sup>34,63–68</sup> Very recently, Zarrougui et al.<sup>63</sup> examined transport and thermodynamic properties of ethylammonium nitrate [EAN] with water as a function of temperature. Later, thermophysical properties of aqueous solution of ammonium-based ILs such as diethylammonium acetate [DEAA], triethylammonium acetate [TEAA], diethylammonium hydrogen sulfate [DEAS], triethylammonium hydrogen sulfate [TEAS], trimethylammonium

**Received:** May 14, 2015

**Revised:** August 24, 2015

**Accepted:** August 25, 2015

**Published:** August 25, 2015

**Table 1.** Molecular Mass (MW), Solvent Purity, Density ( $\rho$ ), Speed of Sound ( $u$ ), Viscosity ( $\eta$ ), and Refractive Index ( $n_D$ ) for the Solvents such as Ammonium-Based ILs and Water at  $T = 25\text{ }^\circ\text{C}$ 

solvent	MW (g mol <sup>-1</sup> )	% purity	$\rho$ (g·cm <sup>-3</sup> )		$u$ (m·s <sup>-1</sup> )		$\eta$ (m·Pa·s)		$n_D$	
			exptl	lit.	exptl	lit.	exptl	lit.	exptl	lit.
water	18.02	99	0.99704	0.99704 <sup>a</sup>	1496	1496 <sup>a</sup>	0.89	0.89 <sup>a</sup>	1.331	1.330 <sup>a</sup>
[TMAH]	91.10	99	1.01797	1.01797 <sup>b,c,d</sup>	1828	1828 <sup>b,c,d</sup>	2.77	2.77 <sup>b,c</sup>	1.387	–
[TEAH]	147.16	99	1.00881	1.00881 <sup>b,c,d</sup>	1814	1814 <sup>b,c,d</sup>	4.94	4.94 <sup>b,c</sup>	1.374	–
[TPAH]	203.25	99	0.99594	0.99594 <sup>b,c,d</sup>	1801	1801 <sup>b,c,d</sup>	6.10	6.10 <sup>b,c</sup>	1.412	–
[TBAH]	259.34	99	0.99358	0.99358 <sup>b,c</sup>	1798	1798 <sup>b,c</sup>	6.69	6.69 <sup>b,c</sup>	1.407	–

<sup>a</sup>Ref 34. <sup>b</sup>Ref 70. <sup>c</sup>Ref 71. <sup>d</sup>Ref 72

acetate [TMAA], and trimethylammonium hydrogen sulfate [TMAS] were reported over a wide composition range by Umaphathi et al.<sup>34</sup> Taib and Murugasen<sup>67</sup> reported the density and excess volumes for bis(2-hydroxyethyl) ammonium acetate with water over the entire composition range. Alvarez et al.<sup>64</sup> reported  $\rho$  and  $u$  data for 2-hydroxyethylammonium acetate with water in the whole concentration range at different temperatures from 15 to 50 °C. Further, the Xu research group carried out the measurement of the thermophysical properties of ethylammonium acetate with water<sup>65</sup> and *n*-butylammonium acetate or *n*-butylammonium nitrate with water<sup>66</sup> over the whole concentration range. Most of these works have explicitly elucidated the influence of anions of ammonium-based ILs on the thermophysical properties. However, the effects of the length of the cation alkyl chains in the aqueous solution of ammonium-based ILs are scarcely studied. To shed some light on this subject, in the present work the thermophysical properties of a series of ammonium-based ILs possessing tetraalkylammonium cation [R<sub>4</sub>N]<sup>+</sup> having fixed hydroxide anion [OH]<sup>-</sup> with water in the temperature range from 25 to 40 °C and over the whole composition range of ILs are studied.

This work reports the measured thermophysical properties such as density ( $\rho$ ), speed of sound ( $u$ ), viscosity ( $\eta$ ), and refractive index ( $n_D$ ) as well as derived properties, i.e., excess molar volume ( $V^E$ ), deviation in isentropic compressibility ( $\Delta\kappa_s$ ), deviation in viscosity ( $\Delta\eta$ ), and deviation in refractive index ( $\Delta n_D$ ) for four ammonium-based ILs, such as tetramethylammonium hydroxide [TMAH], tetraethylammonium hydroxide [TEAH], tetrapropylammonium hydroxide [TPAH], and tetrabutylammonium hydroxide [TBAH] with water over the entire composition range of IL at various temperatures and under atmospheric pressure. The data were correlated by the Redlich–Kister polynomial equation.<sup>70</sup> Finally, the conductor-like screening model for real solvents (COSMO-RS) is used to gather further knowledge of the water–IL molecular interactions.

## 2. EXPERIMENTAL SECTION

**2.1. Materials.** All four ammonium-based ILs used in the present study—[TMAH], [TEAH], [TPAH], and [TBAH]—were synthesized in our laboratory. We have used <sup>1</sup>H NMR techniques to characterize the ILs, and the detailed information was reported in our previous paper.<sup>70</sup> The purity of the water and ILs was checked by measuring the  $\rho$ ,  $u$ ,  $\eta$ , and  $n_D$ , which are in good agreement with literature values.<sup>34,70–72</sup> All the ILs—[TMAH], [TEAH], [TPAH], and [TBAH]—had low levels of water (below 70 ppm) as analyzed by Karl Fischer titrator from Analab (Micro Aqua Cal 100). High-purity water was obtained from Nano pure-Ultra pure Water Equipment (Rions, New Delhi), which was distilled and deionized with a

resistivity of 18.3 Ω·cm of pure water at 25 °C for making the aqueous IL solutions. The values of  $\rho$ ,  $u$ ,  $\eta$ , and  $n_D$  of pure substances at 25 °C are collected in Table 1.

**2.2. Methods and Procedure.** The samples were prepared by weighing the components using a Mettler Toledo balance with an accuracy of  $\pm 0.0001$  g for all measurements.<sup>70</sup> The estimated uncertainty on the mole fraction was found to be less than  $5 \times 10^{-4}$ . After the sample was mixed, the bubblefree homogeneous sample was transferred into the U-tube of the densimeter or the sample cell of ultrasonic interferometer or refractometer through a medical syringe.<sup>71</sup> A bubblefree sample was introduced into the sample cell, and the cell was placed under the sensor plates of the viscometer for  $\eta$  measurements.<sup>71</sup>

Density measurements of ILs, water, and IL–water were measured using an Anton-Paar DMA-4500 M vibrating-tube densimeter with a temperature accuracy of  $\pm 0.03$  °C. The uncertainties in the  $\rho$  measurements were  $\pm 0.00005$  g·cm<sup>-3</sup>. The instrument was calibrated once a day with double distilled, deionized water and with air at 20 °C as standards.<sup>71</sup> At least three independent measurements were performed at each temperature. A single-crystal ultrasonic interferometer (Model F-05) from Mittal Enterprises, New Delhi, India, at fixed 2 MHz frequency was used for  $u$  measurements for pure solvents and mixtures at various temperatures.<sup>71</sup> The uncertainty of the sound velocity is 0.02%.

A Vibro viscometer (model SV-10, A&D Company Limited, Japan) was used for  $\eta$  measurements, and the detailed procedure was explained in our previous paper.<sup>71</sup> Typically, the viscosity uncertainty is 1%. The refractive index was determined using Abbe refractometer from Mittal Enterprises, New Delhi, India, with an accuracy of  $\pm 0.0002$ . Refractometer was calibrated by measuring the  $n_D$  values of the high-purity water and purified methanol at various temperatures. A thermostatically controlled, well-stirred circulating water bath with a temperature controlled to  $\pm 0.01$  °C was used for the measurements of thermophysical parameters such as  $u$ ,  $\eta$ , and  $n_D$  of the binary mixtures.<sup>71</sup>

## 3. THEORETICAL BASIS

**3.1. COSMO-RS.** The COSMO-RS is a novel quantum chemical approach to describe the chemical potential in the liquid phase and has become a frequently used alternative to force field-based molecular simulation methods on one side and group-contribution methods on the other. The COSMO-RS model is the most progressive kind of a dielectric model where molecules are placed in a conductor as the reference state.<sup>73</sup> Through its unique combination of a quantum chemical treatment of solutes and solvents with an efficient statistical thermodynamics procedure for the molecular surface interactions, it enables the efficient calculation of phase equilibrium

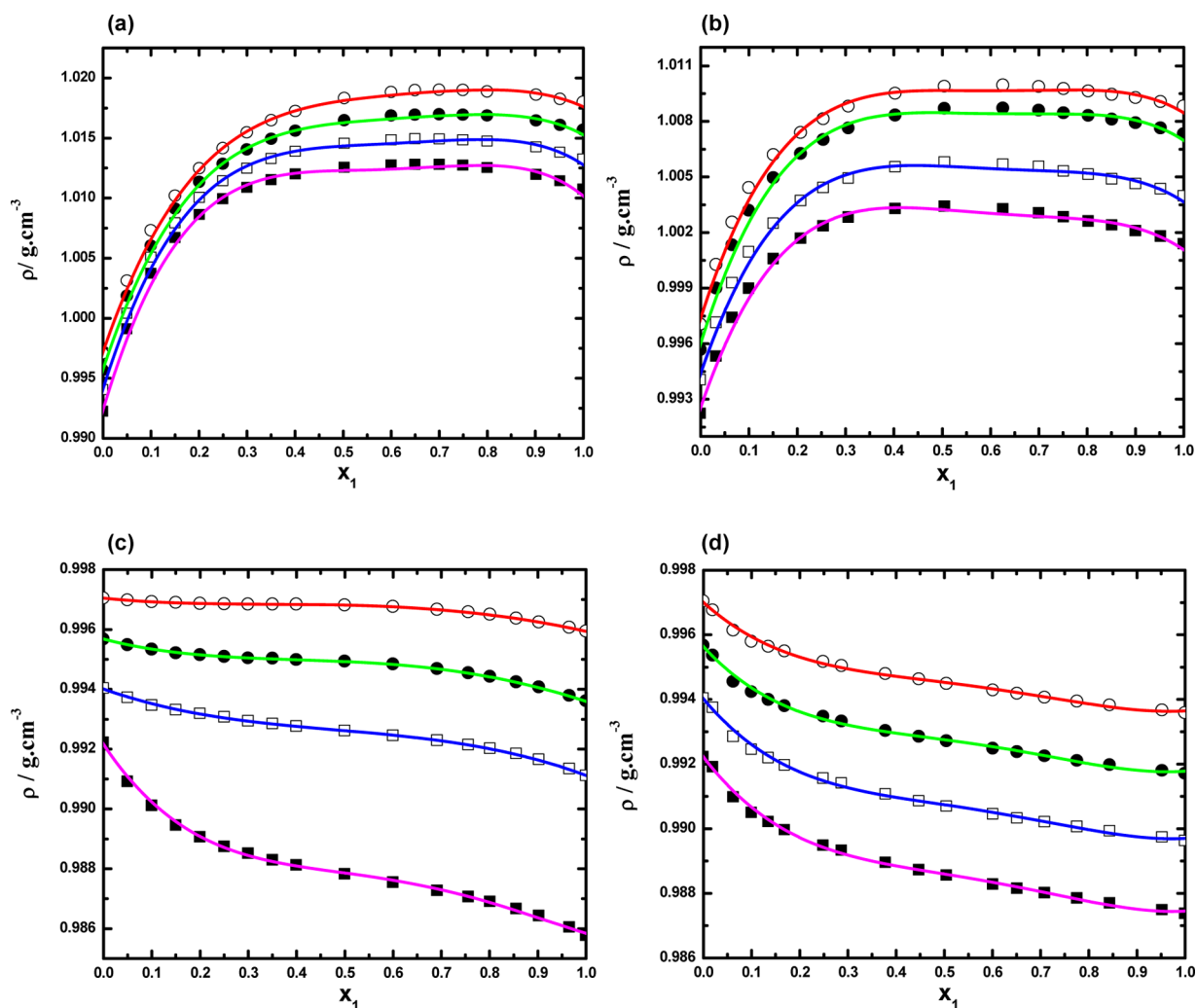


**Figure 1.** Densities ( $\rho$ ) for the mixtures of ILs with water vs mole fraction of IL ( $x_1$ ) for (a) [TMAH] + water, (b) [TEAH] + water, (c) [TPAH] + water, and (d) [TBAH] + water ( $x_2$ ) at 25 °C (○), 30 °C (●), 35 °C (□), and 40 °C (■). The solid lines show the smoothness of the data.

and other thermodynamic properties. The detailed theory on COSMO-RS can be found in the original work by Klamt.<sup>35,74</sup>

The standard procedure of COSMO-RS calculations consists of two steps. First, the software TURBOMOLE 6.1 program package at the RI-DFT BP/TZVP level is used for the quantum-chemical calculation to generate the COSMO files for each studied compound.<sup>75</sup> To achieve better and comprehensive computation results, only conformations with the least energy, i.e., most stable conformer, were considered. The three-dimensional (3D) distribution of the screening charge density on the surface of each molecule is converted into a surface composition function, called the sigma profile ( $\sigma$ -profile),  $p(\sigma)$ . Then COSMO-RS calculations are performed in the COSMOtherm software using the parameter file BP\_TZVP\_C30\_1401 (COSMO logic GmbH & Co KG, Leverkusen, Germany).<sup>35,76,77</sup> Following the two-step procedure, COSMO-RS models have been applied and proved to be an excellent tool to evaluate qualitatively the strength of the interactions established by ILs with other compounds. The detailed calculation and procedure of estimating activity coefficients using COSMO-RS can be found elsewhere,<sup>78,79</sup> and the procedure for estimating excess enthalpies can be also found in the literature.<sup>35,75</sup>

#### 4. RESULTS AND DISCUSSION

The molecular interactions between unlike molecules of liquid mixtures depend on the nature and structural conformations of the components.<sup>71</sup> Our choice of several tetraalkylammonium-based cations and hydroxide as common anion of ILs is aimed at studying the effect of the alkyl chain length of the cation on the interactions with water at different temperatures.<sup>35</sup> In this regard, we have measured the thermophysical properties  $\rho$ ,  $u$ ,  $\eta$ , and  $n_D$  over the entire composition range of ILs at temperatures ranging from 25 to 40 °C in steps of 5 °C under atmospheric pressure. The experimental values of  $\rho$ ,  $u$ ,  $\eta$ , and  $n_D$  are graphically represented in Figures 1–4 and reported in Table 1S at all investigated temperatures as a function of IL concentration. Figure 1 reveals that the  $\rho$  values of ammonium-based ILs with water do not follow the same trend. In the binary mixtures of [TMAH] and [TEAH] with water,  $\rho$  values initially increase up to  $x_1 \approx 0.6500$ – $0.7000$  at all experimental temperatures; later, the values slightly decrease with increasing concentration of IL, as shown in panels a and b of Figure 1, respectively. This may be due to the progressive association of the ion–ion pair interactions between [TMAH] or [TEAH] with water up to the  $x_1 \approx 0.6500$ – $0.7000$ , respectively, later the results attributed to the weakening of the ion–ion pair interactions. On the other hand, the  $\rho$  values for the binary

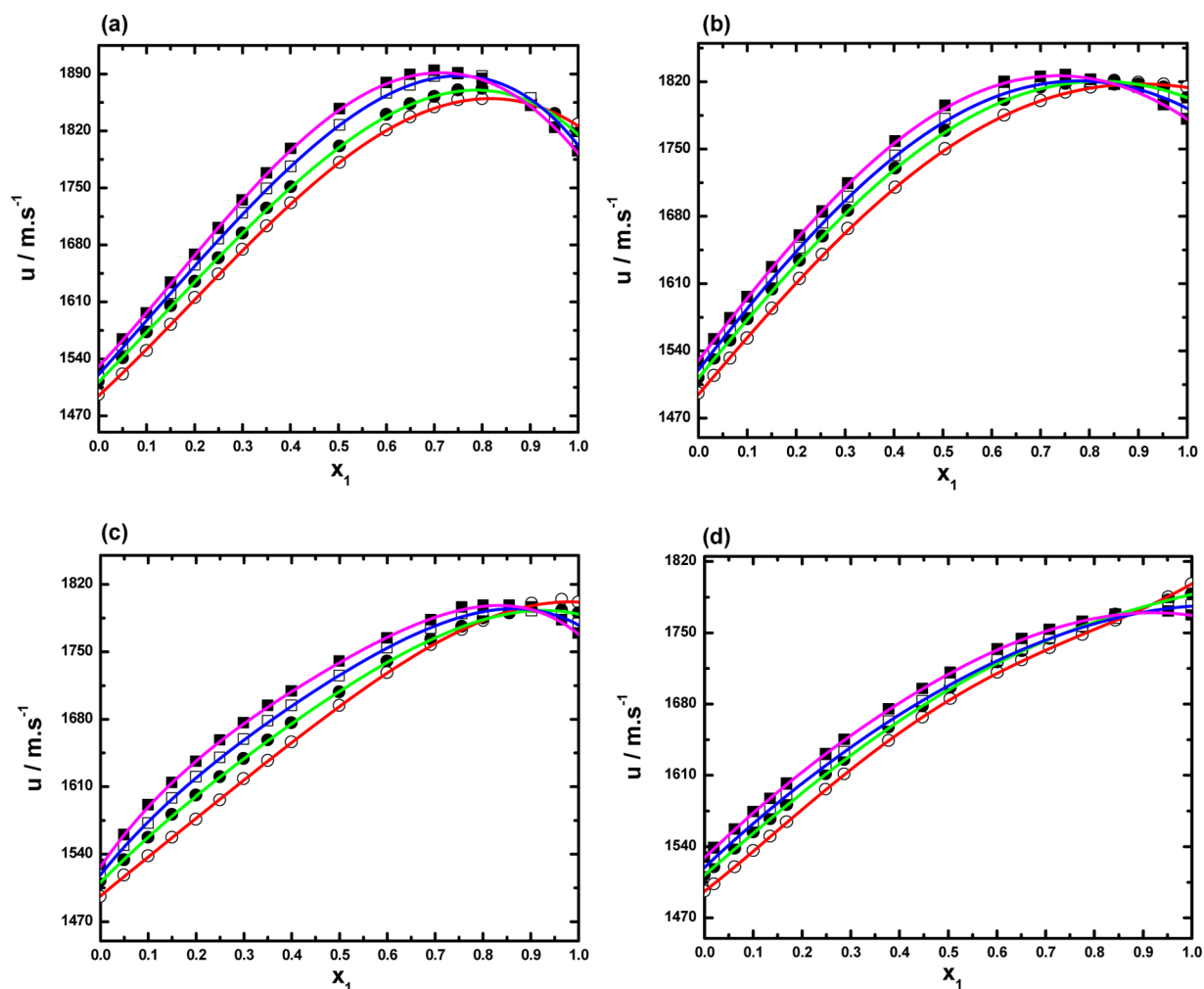


**Figure 2.** Speed of sound ( $u$ ) for the mixtures of ILs with water vs mole fraction of IL ( $x_1$ ) for (a) [TMAH] + water, (b) [TEAH] + water, (c) [TPAH] + water, and (d) [TBAH] + water ( $x_2$ ) at 25 °C (○), 30 °C (●), 35 °C (□), and 40 °C (■). The solid lines represent the smoothness of the data.

mixture of [TPAH] or [TBAH] with water monotonically decrease at all experimental temperatures with increasing mole fraction of the IL, as can be seen in panels c and d of Figure 1, respectively. This may be due to the weakening of the ion–ion pair interactions between [TPAH] or [TBAH] with water. However, the increase or decrease of the  $\rho$  values of the liquid mixtures depends upon increase of the cation alkyl chain length from methyl to butyl of ammonium-based ILs. The data in Figure 1 indicates that the  $\rho$  values of the ILs follow the order [TMAH] > [TEAH] > [TPAH] > [TBAH], which shows that the lower alkyl chain length of cation of ILs is much denser than larger alkyl chain length of ILs. This may be due to the ion–ion pair interactions decreasing with increasing size of alkyl chain length of cation of the ILs.

The  $u$  values of four ammonium-based ILs with water were measured at various temperatures, and these data are displayed in Figure 2 as a function of IL concentration. As illustrated in Figure 2, we have also observed that the  $u$  values increase with temperature. The values of  $u$  for the [TMAH]–water system increase sharply up to  $x_1 \approx 0.8000$  of [TMAH] after which an abrupt decrease in  $u$  values with increasing concentration of [TMAH] is observed. On the other hand,  $u$  values for [TEAH] or [TPAH] and water (Figure 2b,c) increase up to  $x_1 \approx 0.9000$  of ILs, respectively; above this concentration, the  $u$  values

decrease at all investigated temperatures. As shown in Figure 2d, the [TBAH]–water system gives a monotonic increase in  $u$  values when the concentration of TBAH increases. The order of  $u$  values of ammonium-based ILs with water is [TMAH] > [TEAH] > [TPAH] > [TBAH]. This order indicates that the interaction with water of the lower alkyl chain length cation ILs is stronger than that of the higher alkyl chain length ILs. This may be due to the stronger molecular interactions decreasing with increasing size of alkyl chain length of the cation of ammonium-based ILs.

Furthermore, we have measured the  $\eta$  values for [TMAH], [TEAH], [TPAH], and [TBAH] with water under the same experimental conditions, and the results are presented in Figure 3. Here, the  $\eta$  values of each IL mixture with water are shown to increase with the composition of IL at all studied temperatures, whereas  $\eta$  values decrease as the temperature increases for all the systems. The data in Figure 3 indicates that the  $\eta$  values of the ILs follow the order [TMAH] < [TEAH] < [TPAH] < [TBAH]. The  $\eta$  values increase with increasing alkyl side chain length of the cation of ILs. These results indicate the strong interactions between the ions of the ILs with the water.

To obtain further insight into the role of ILs in the molecular interactions with water,  $n_D$  measurements were carried out for all four ammonium-based ILs with water under the same

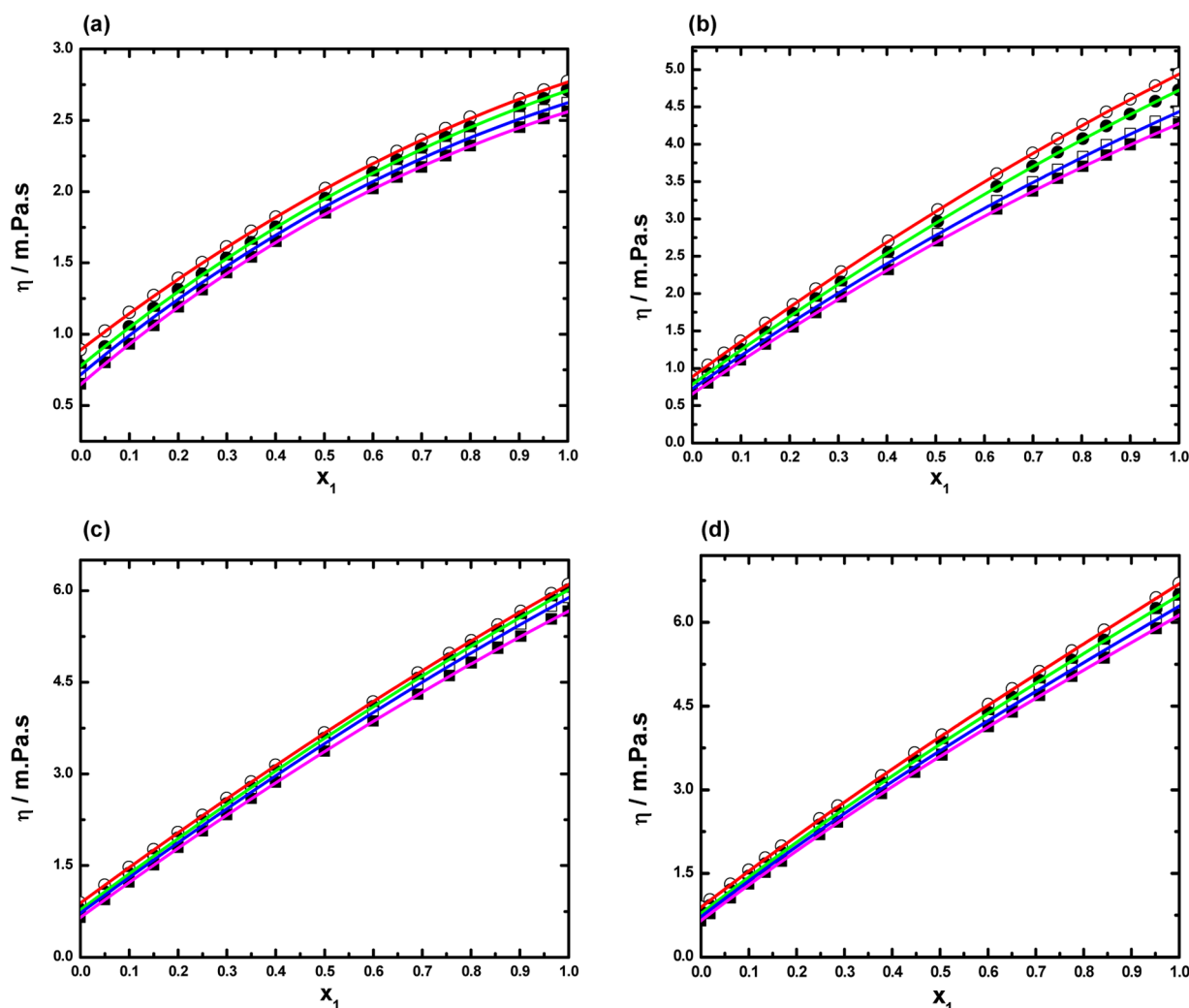


**Figure 3.** Viscosities ( $\eta$ ) for the mixtures of ILs with water vs mole fraction of IL ( $x_1$ ) for (a) [TMAH] + water, (b) [TEAH] + water, (c) [TPAH] + water, and (d) [TBAH] + water ( $x_2$ ) at 25 °C (○), 30 °C (●), 35 °C (□), and 40 °C (■). The solid lines represent the smoothness of the data.

experimental conditions, and the values are graphically represented in Figure 4. The  $n_D$  values for ILs with water mixtures increase with increasing composition of IL. However, Figure 4 reveals that the  $n_D$  values increase up to  $x_1 \approx 0.9000$  or  $x_1 \approx 0.8000$  for [TMAH] or [TEAH] and water systems, respectively. Then the  $n_D$  values slightly decrease with further increases of the composition of [TMAH] or [TEAH]. In the case of [TEAH]–water, the  $n_D$  values slightly decrease as compared to that of [TPAH] or [TBAH] after  $x_1 \approx 0.9000$  because of the +inductive effect (+I effect) by short alkyl chain length of cation ILs is weaker than that of large alkyl chain length of cation ILs at these IL concentrations in water.<sup>71</sup> This indicates that the lower +I effect of [TEAH] forms weaker interactions with water as compared to greater +I of other ILs such as [TPAH] or [TBAH] at high concentrations. The order of  $n_D$  values for all four ILs with water showed the following trend: [TPAH] > [TBAH] > [TMAH] > [TEAH]. This order indicates that  $n_D$  values of ILs with water do not follow the regular trend. On the other hand, Figure 4c,d shows that the  $n_D$  values increase with the mole fraction of [TPAH] or [TBAH] in the water.

Our results clearly show that addition of water to ILs can bring significant changes in  $\rho$ ,  $u$ ,  $\eta$ , and  $n_D$  of the ILs. For understanding the effect of water on the thermophysical

properties of the ammonium-based ILs, we have further evaluated  $V^E$ ,  $\Delta\kappa_s$ ,  $\Delta\eta$ , and  $\Delta n_D$  values from well-known thermodynamic relations.<sup>70–72</sup> The composition dependence of the  $V^E$ ,  $\Delta\kappa_s$ ,  $\Delta\eta$ , and  $\Delta n_D$  properties represent the deviation from ideal behavior of the mixtures and provide an indication of the interactions between ammonium-based ILs and water; these values are included in Table 1S.

The following Redlich–Kister expression was used to correlate these properties:

$$Y = x_1 x_2 \left( \sum_{i=0}^n a_i (x_1 - x_2)^i \right) \quad (1)$$

where  $Y$  refers to  $V^E$ ,  $\Delta\kappa_s$ ,  $\Delta\eta$ , or  $\Delta n_D$  and  $x_1$  and  $x_2$  are the mole fractions of pure compounds 1 and 2, respectively.  $a_i$  is an adjustable parameter that can be obtained by least-squares analysis. The values of  $a_i$  are collected in Table 2S along with standard deviations of the fit.

The  $V^E$  values of four ILs and water systems are graphically represented in Figure 5 at different temperatures. The  $V^E$  values are negative in the whole concentration region with a minimum  $x_1 \approx 0.5000$ , 0.5500, 0.6600, and 0.4500 for [TMAH], [TEAH], [TPAH], and [TBAH] with water, respectively (Figure 5). The  $V^E$  values become more negative with

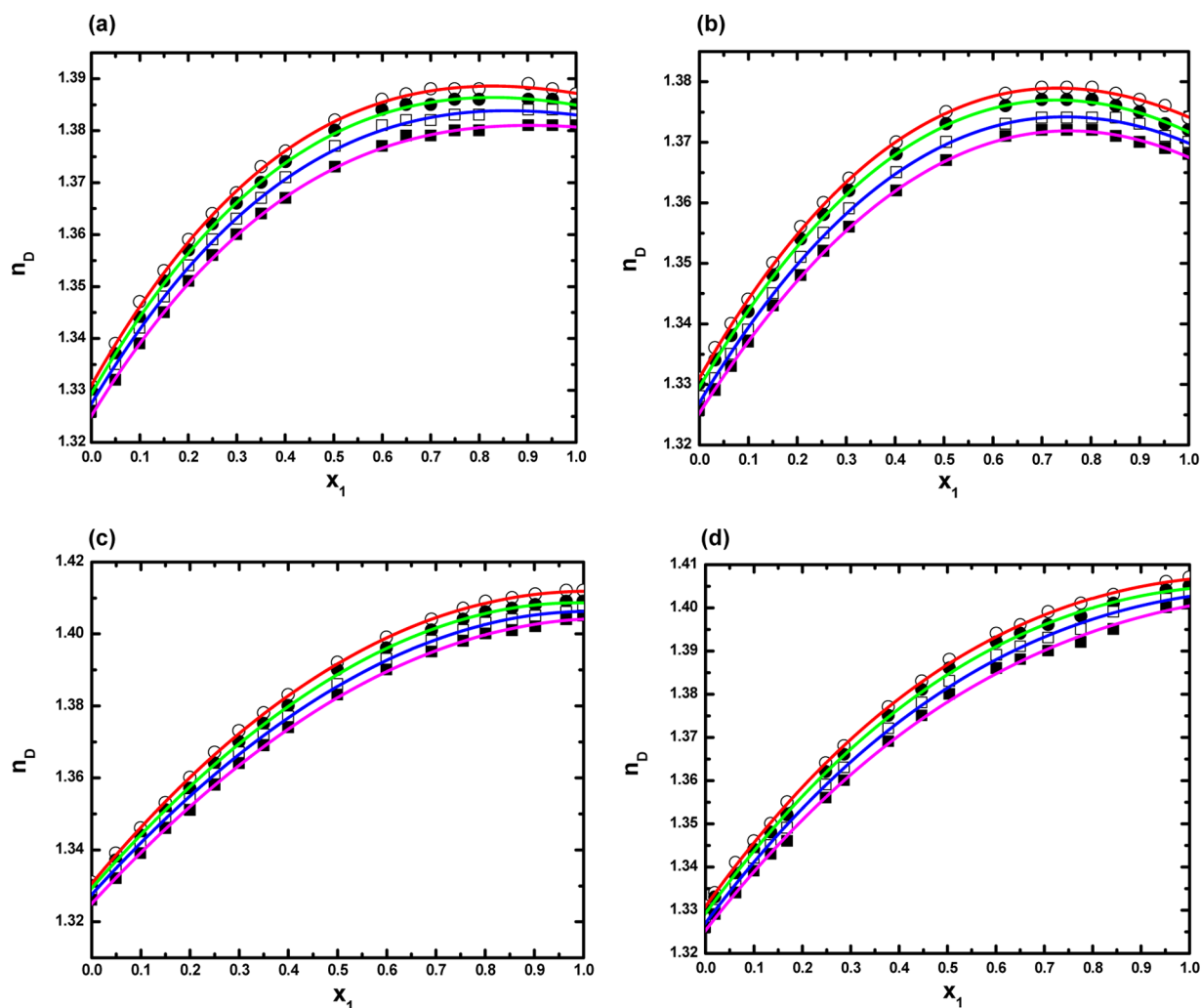


**Figure 4.** Refractive indices ( $n_D$ ) for the mixtures of ILs with water vs mole fraction of IL ( $x_1$ ) for (a) [TMAH] + water, (b) [TEAH] + water, (c) [TPAH] + water, and (d) [TBAH] + water ( $x_2$ ) at 25 °C (○), 30 °C (●), 35 °C (□), and 40 °C (■). The solid lines represent the smoothness of the data.

increasing temperature from 25 to 40 °C for all the mixtures, and this is because of formation of the hydrogen bonds between water molecules and ILs. The negative  $V^E$  values show that a more efficient packing or attractive interactions occur when these ILs are mixed with water. The more negative  $V^E$  values suggest the formation of stronger association interactions between the ions of IL and water molecules. These interactions are shown schematically in Scheme 1. Thus, on the basis of  $V^E$  values, it can be concluded that the order of the interactions for binary mixtures of water with ILs follow the sequence [TMAH] > [TEAH] > [TPAH] > [TBAH]. Therefore, on the basis of this order, we observed that for lower cation alkyl chain length the ILs interact with water more strongly than those with longer alkyl chains. The explanation is probably due to the larger steric hindrance of the alkyl chain in [TPAH] or [TBAH] IL. Furthermore, the higher alkyl chain molecules decrease the hydrogen bonding tendency between [TPAH] or [TBAH] with water molecules because of its structural effects. This, it is important to note that the nature of interactions in the IL–water system is highly dependent on the size and nature of the cation of the IL.<sup>70</sup> The negative values of the  $V^E$  observed for the ILs in water indicate that there may be stronger intermolecular interactions between the ions of ILs and polar

species, i.e., a more efficient packing and/or attractive interaction occurred when ILs and the water molecules were mixed. Unlike nonelectrolyte/organic solvent and water mixtures, the IL–water systems comprise various ions which do not retain their individual nature; therefore, the interactions in such mixtures are quite complex.<sup>70–72,80–82</sup>

One of the important features of the COSMO-RS methodology is that it provides the three-dimensional polarized charge distribution ( $\sigma$ , sigma) on the molecular surface, easily visualized on the histogram function  $\sigma$ -profile as depicted in Figure 6, which can be used to understand the polarity of the compounds and their interactions with a solvent. The  $\sigma$ -profile of water is very broad; on its negative side, water shows a broad peak at about  $-1.6 \text{ e}\cdot\text{nm}^{-2}$  resulting from the two polar hydrogen atoms, while on the positive side, the same broad peak at  $1.8 \text{ e}\cdot\text{nm}^{-2}$  resulting from the lone pairs of the oxygen atom. Both peaks lie beyond the threshold ( $\sigma_{\text{hb}} = \pm 0.79 \text{ e}\cdot\text{nm}^{-2}$ ), which means that large parts of the surface of water molecules are able to form more or less strong hydrogen bonds. Both H-bond acceptors and donors can undergo efficient H-bonding in water if they overcome this threshold.<sup>35</sup> The same amount of strongly positive and equally strong

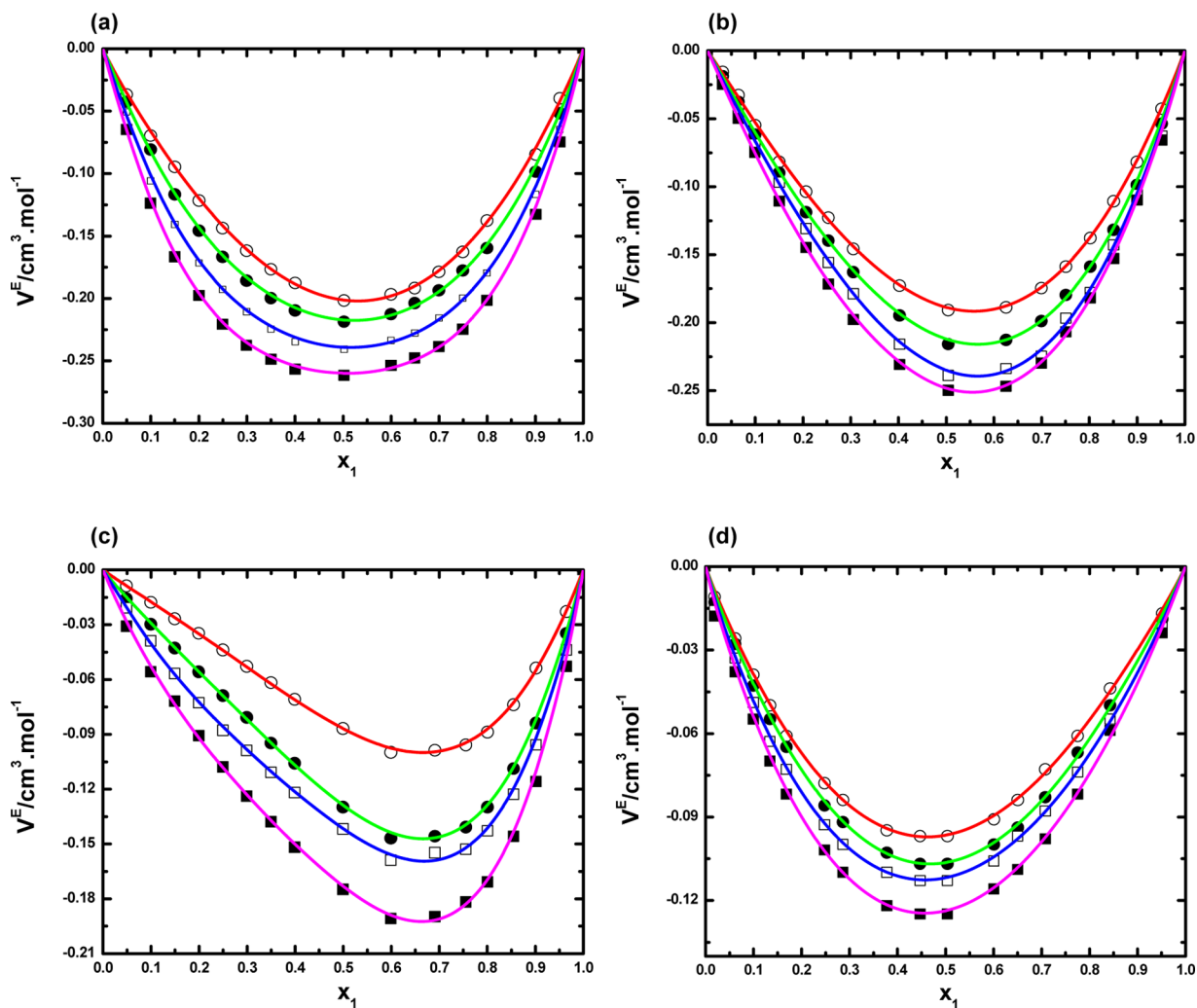


**Figure 5.** Excess volumes ( $V^E$ ) for the mixtures of ILs with water vs mole fraction of IL ( $x_1$ ) for (a) [TMAH] + water , (b) [TEAH] + water , (c) [TPAH] + water, and (d) [TBAH] + water ( $x_2$ ) at 25 °C (○), 30 °C (●), 35 °C (□), and 40 °C (■). Redlich–Kister correlations are plotted as solid lines.

**Scheme 1. Schematic Depiction of Hydrogen Bonding and Ion-Pair Interactions between Water and Ions of Ammonium-Based ILs**

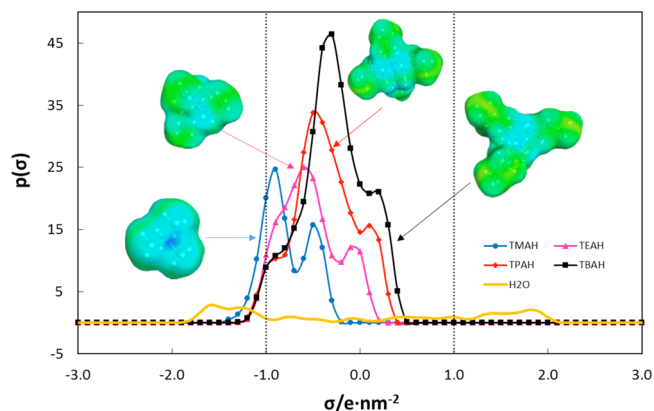
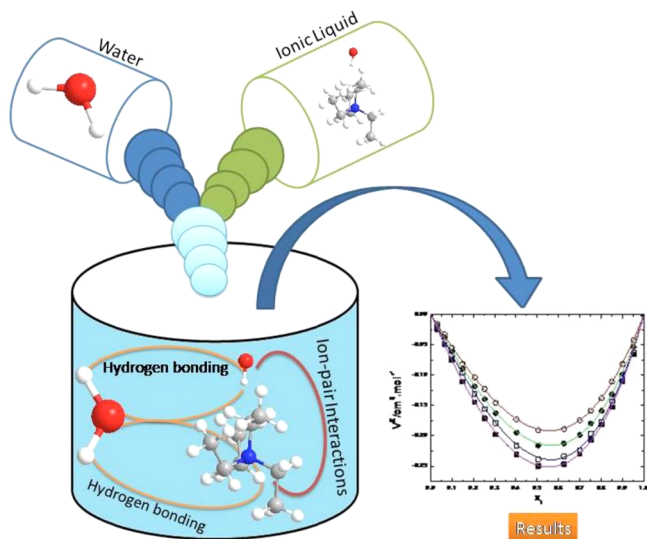


**Figure 6.** Sigma profile of [TMAH] (●), [TEAH] (▲), [TPAH] (◆), [TBAH] (■), and H<sub>2</sub>O (line).

negative surface area enables energetically very favorable pairing of positive and negative surfaces and the formation of strong hydrogen bonding.<sup>35</sup> As evident from Figure 6, the nonpolar area increases from tetramethylammonium cation [TMA]<sup>+</sup> to tetrabutylammonium cation [TBA]<sup>+</sup> because of the increase in

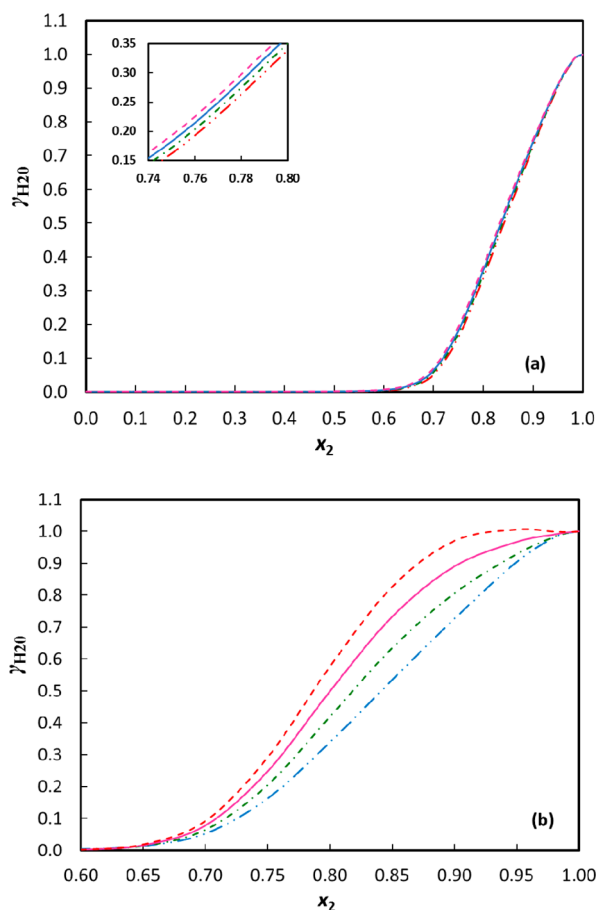


**Figure 7.** Activity coefficient of water,  $\gamma_{H_2O}$ , as a function of concentration of water for (a) [TMAH] at studied temperatures (25 °C (dash-dot-dot line), 30 °C (dash-dot line), 35 °C (solid line), and 40 °C (dashed line)) and (b) for studied IL [TMAH] (dash-dot-dot line), [TEAH] (dashed dot), [TPAH] (solid line), and [TBAH] (dashed line) at 25 °C predicted by COSMO-RS.

the alkyl chain length, which makes the interaction of [TBAH] with water the weakest.

Activity coefficients of water in the studied IL system predicted from COSMO-RS presents negative deviations to the ideality, confirming the favorable interactions with water, with the order [TMAH] > [TEAH] > [TPAH] > [TBAH].

This interaction behavior based on activity coefficient predicted by COSMO-RS at different temperatures (Figure 7a) and also at fixed temperature for different studied ILs (Figure 7b) (for other temperatures and ILs, see Figure S1 of Supporting Information) have been found to be the same interaction behavior compared with that studied using the experimental results of  $\rho$ ,  $u$ ,  $\eta$ , and  $n_D$  as well as derived properties. The predicted activity coefficients clearly show the effect of the temperature on the studied ILs and also the effect of the various ILs at a given temperature, though in the latter case the impact of variation is more pronounced. An agreement of activity coefficient of water for the studied ILs predicted by COSMO-RS with experimental results gave us confidence to further study the excess enthalpy ( $H^E$ ). According to the COSMO-RS method, the  $H^E$  of the fluid mixture can be predicted by summing the contributions of each component of the mixture.

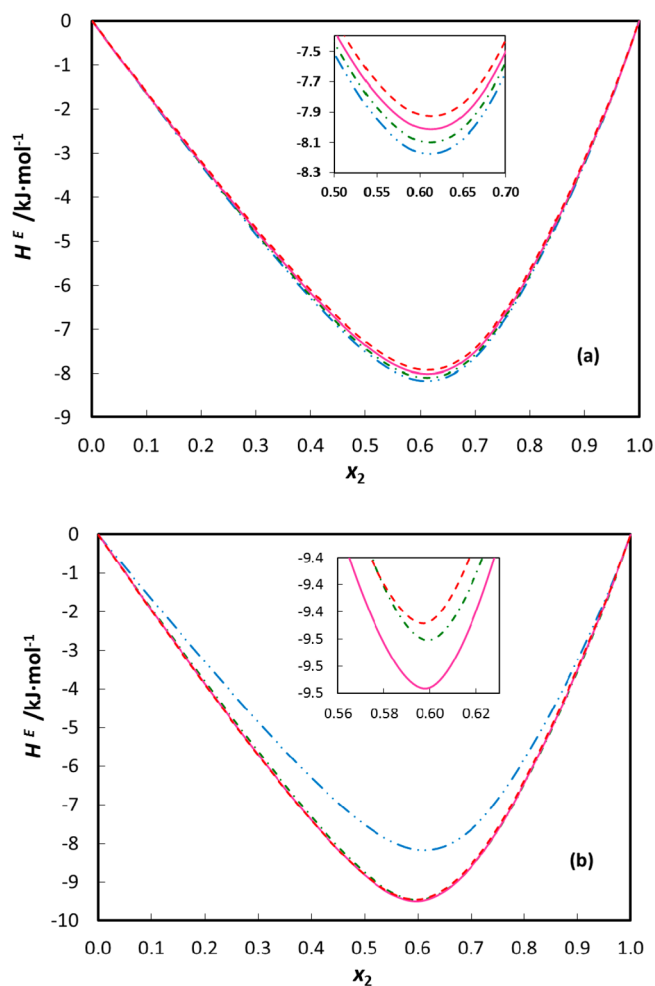


**Figure 8.** Excess enthalpy of binary mixture of (a) [TMAH]–water at studied temperatures (25 °C (dash-dot-dot line), 30 °C (dash-dot line), 35 °C (solid line), and 40 °C (dashed line)) and (b) for studied ILs [TMAH] (dash-dot-dot line), [TEAH] (dash-dot line), [TPAH] (solid line), and [TBAH] (dashed line) at 25 °C predicted by COSMO-RS.

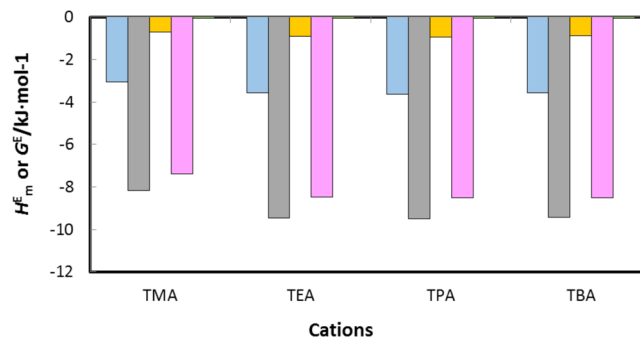


**Figure 9.** Total predicted excess free Gibbs energy,  $G^E$  (blue bars), and  $H^E$  (gray bars) of water–IL binary mixture at 25 °C using COSMO-RS at  $x_2 = 0.5000$  in terms of contribution of  $H_{MF}^E$  (yellow bars),  $H_{MB}^E$  (pink bars), and  $H_{vdW}^E$  (green bars) to the total excess enthalpy,  $H^E$ .

$$H^E = \sum x_i H_i^E = \sum x_i [H_{(i,mix)} - H_{(i,pure)}] \quad (2)$$

where  $H_i^E$  is the excess enthalpy of each component of the mixture, which is defined as the difference between the enthalpy of molecule  $i$  in the mixture and in the pure state. In the COSMO-RS model, the excess enthalpy of a binary

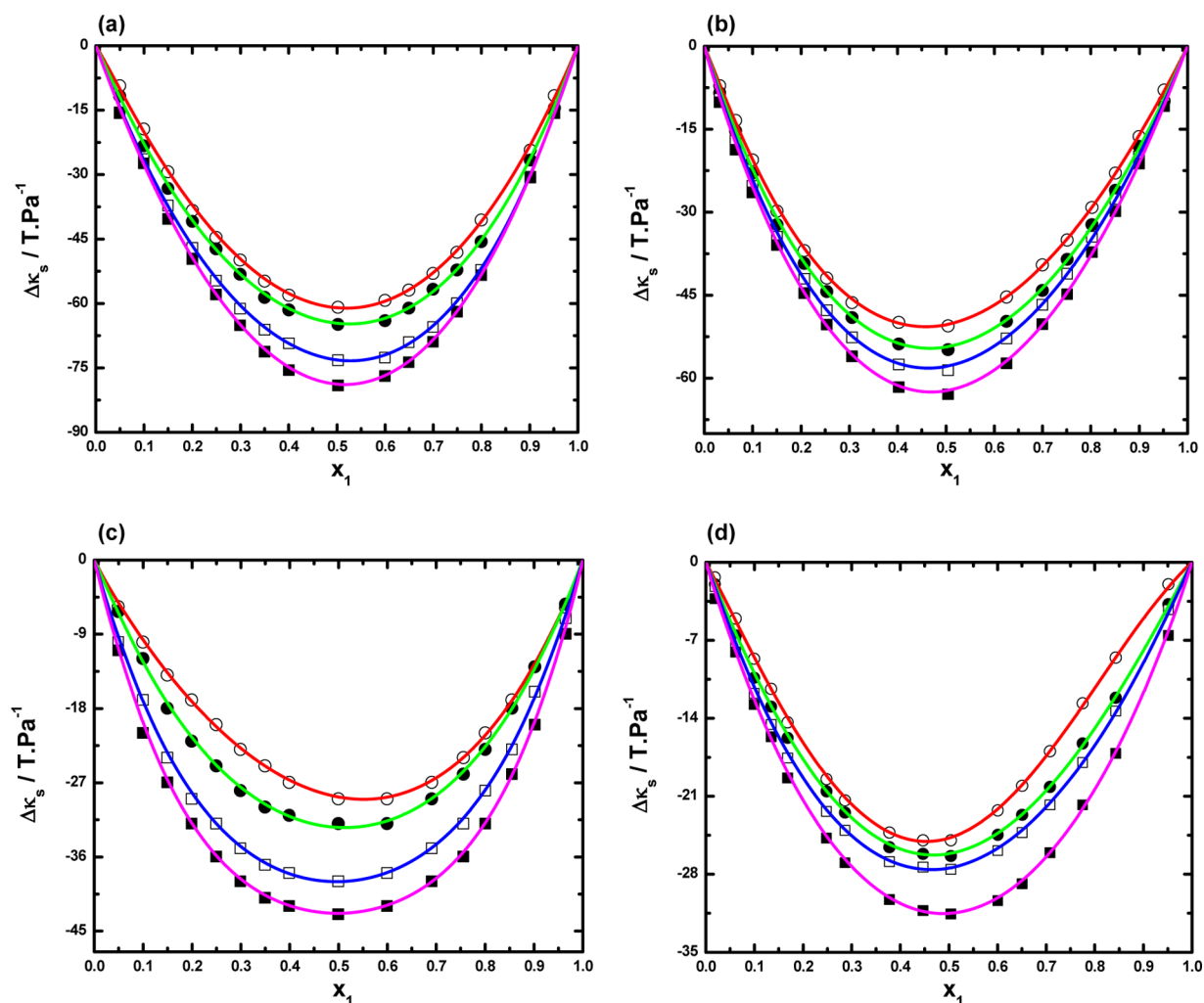


**Figure 10.** Deviation in isentropic compressibilities ( $\Delta\kappa_s$ ) for the mixtures of ILs with water vs mole fraction of IL ( $x_1$ ) for (a) [TMAH] + water, (b) [TEAH] + water, (c) [TPAH] + water, and (d) [TBAH] + water ( $x_2$ ) at 25 °C (○), 30 °C (●), 35 °C (□), and 40 °C (■). Redlich–Kister correlations are plotted as solid lines.

mixture is the algebraic sum of each specific contribution such as hydrogen bonding, van der Waals forces, and misfit.

$$H^E = H^E(\text{H-bond}) + H^E(\text{vdW}) + H^E(\text{misfit}) \quad (3)$$

Combing eqs 2 and 3, we get

$$H^E = \sum H_i^E(\text{H-bond}) + \sum H_i^E(\text{vdW}) + \sum H_i^E(\text{misfit}) \quad (4)$$

The binary mixtures of IL and water are mainly characterized by two types of interactions, i.e., structure-making and/or structure-breaking. In our studied system, the interactions are structure-making as apparent from negative  $V^E$  (Figure 5) and negative  $H^E$  (Figure 8) at various temperatures (for others, see Supporting Information Figures S2 and S3). The negative deviation in these studied systems was due to the interstitial accommodation and strong intermolecular interactions, such as electrostatic, van der Waals, and hydrogen bonding.

The predicted negative  $H^E$  shows favorable interactions between water and the ILs. Contributions of each specific interaction to the total excess enthalpy of the IL and water at all studied temperatures are depicted in Figures S4–S6 of the Supporting Information. The negative contribution of  $H_{MF}^E$  to the total excess enthalpy shows that water reduces the

electrostatic interaction between the cation and the anion of the ILs, which arise from the breakage of hydrogen bonds between  $\text{H}_2\text{O}$ – $\text{H}_2\text{O}$  molecules and cation–anion of the ILs, the establishment of new hydrogen bonds between water and the ILs anion, and higher water concentration between  $\text{H}_2\text{O}$ –cation.<sup>83</sup> Figure 8 (for the binary system of water and ILs) shows a minimum at  $x_2 \approx 0.6000$  (similar to what was observed for the excess volumes) that seems to indicate the formation of a complex between one water molecule and one molecule of the IL. Contribution of each specific interaction of tetramethylammonium cation ( $[\text{TMA}]^+$ ), tetraethylammonium cation ( $[\text{TEA}]^+$ ), tetrapropylammonium cation ( $[\text{TPA}]^+$ ), and tetrabutylammonium cation ( $[\text{TBA}]^+$ ) with water at this concentration is depicted in the Figure 9.

From the literature, it is well-known that the anion is dominant in the interactions that control the water miscibility,<sup>35,84,85</sup> and in our studied systems, hydroxide anion  $[\text{OH}^-]$  being common, the contribution to the differences observed result mainly from the cation of the IL–water system. With an increase in the alkyl substituted chain length from [TMAH] to [TBAH], the  $H^E$  predicted from the COSMO-RS results shows a reverse trend in the order  $[\text{TMAH}] < [\text{TMEH}] < [\text{TMPH}] < [\text{TMBH}]$  from that obtained from the predicted activity coefficient model from COSMO-RS and  $V^E$  from

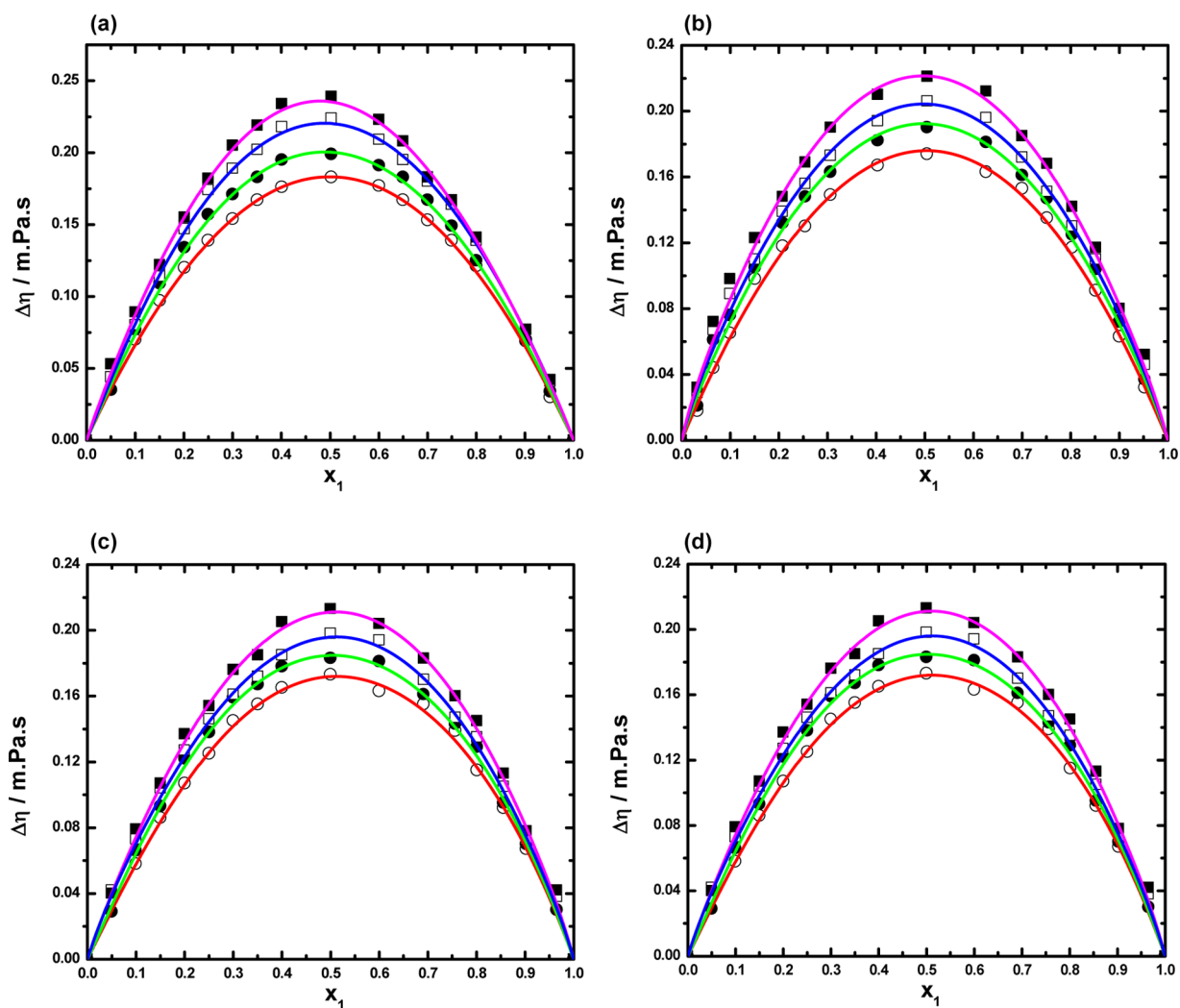


**Figure 11.** Deviation in viscosities ( $\Delta\eta$ ) for the mixtures of ILs with water vs mole fraction of IL ( $x_1$ ) for (a) [TMAH] + water, (b) [TEAH] + water, (c) [TPAH] + water, and (d) [TBAH] + water ( $x_2$ ) at 25 °C (○), 30 °C (●), 35 °C (□), and 40 °C (■) and atmospheric pressure. Redlich–Kister correlations are plotted as solid lines.

experimental results at all studied temperatures, as depicted in Figure 7a (for other temperatures, see Figure S2 of Supporting Information). Also, the  $H^E$  predicted from the COSMO-RS results showed a reverse trend behavior from experimental  $V^E$  for all studied ILs at the different fixed temperatures, as depicted in Figure 7b (for other temperatures, see Figure S3 of Supporting Information). The reverse trend shows that though the reaction process is exothermic, as evident from negative enthalpy values, the process is endothermic and entropically driven. This reverse trend can also be explained from the basic thermodynamic theory of solution. The sign of  $V^E$  agrees with that of  $H^E$ , but in addition, higher  $V^E$ , higher  $H^E$  is not strictly true, as reported earlier in the literature in the case of 1-butyl-3-methylimidazolium and 1-ethyl-3-butyl imidazolium triflate.<sup>86</sup> The same phenomenon was observed in the work of Kurnia et al.<sup>23</sup>

The excess Gibbs free energy was estimated using COSMO-RS using the following equation:

$$\frac{G^E}{RT} = (x_2 \ln \gamma_{H_2O}) + (x_1 \ln \gamma_{IL}) \quad (5)$$

where  $x$  and  $\gamma$  are mole fraction and activity coefficient, respectively. Predicted  $G^E$  for the studied binary mixture gives

negative values (Figure S7 of Supporting Information), which shows spontaneous dissolution of the ILs into water and vice versa, as observed experimentally. Therefore, the COSMO-RS theoretical method used in this study proved to be significant to study the water–IL interactions.

Figure 10 illustrates the  $\Delta\kappa_s$  values over the whole composition range at various temperatures for all the systems as a function of IL concentration. An examination of curves in Figure 10 suggests that  $\Delta\kappa_s$  data are negative for the binary mixtures of [TMAH], [TEAH], [TPAH], and [TBAH] with water over the entire composition range at all the studied temperatures.

The negative  $\Delta\kappa_s$  values of ILs with water are also attributed to the strong attractive interactions due to factors like dipole–dipole interactions between unlike molecules. This may cause an increase in speed of sound and negative deviation in  $\Delta\kappa_s$ . The negative values of  $\Delta\kappa_s$  for the binary mixtures of water with the ILs follow the order [TMAH] > [TEAH] > [TPAH] > [TBAH]. From this order, we have observed that the intermolecular interactions decrease with increasing chain length of alkyl group cation.

The more negative  $\Delta\kappa_s$  values for methyl cation of ILs serve as further evidence that the interactions between small sizes of

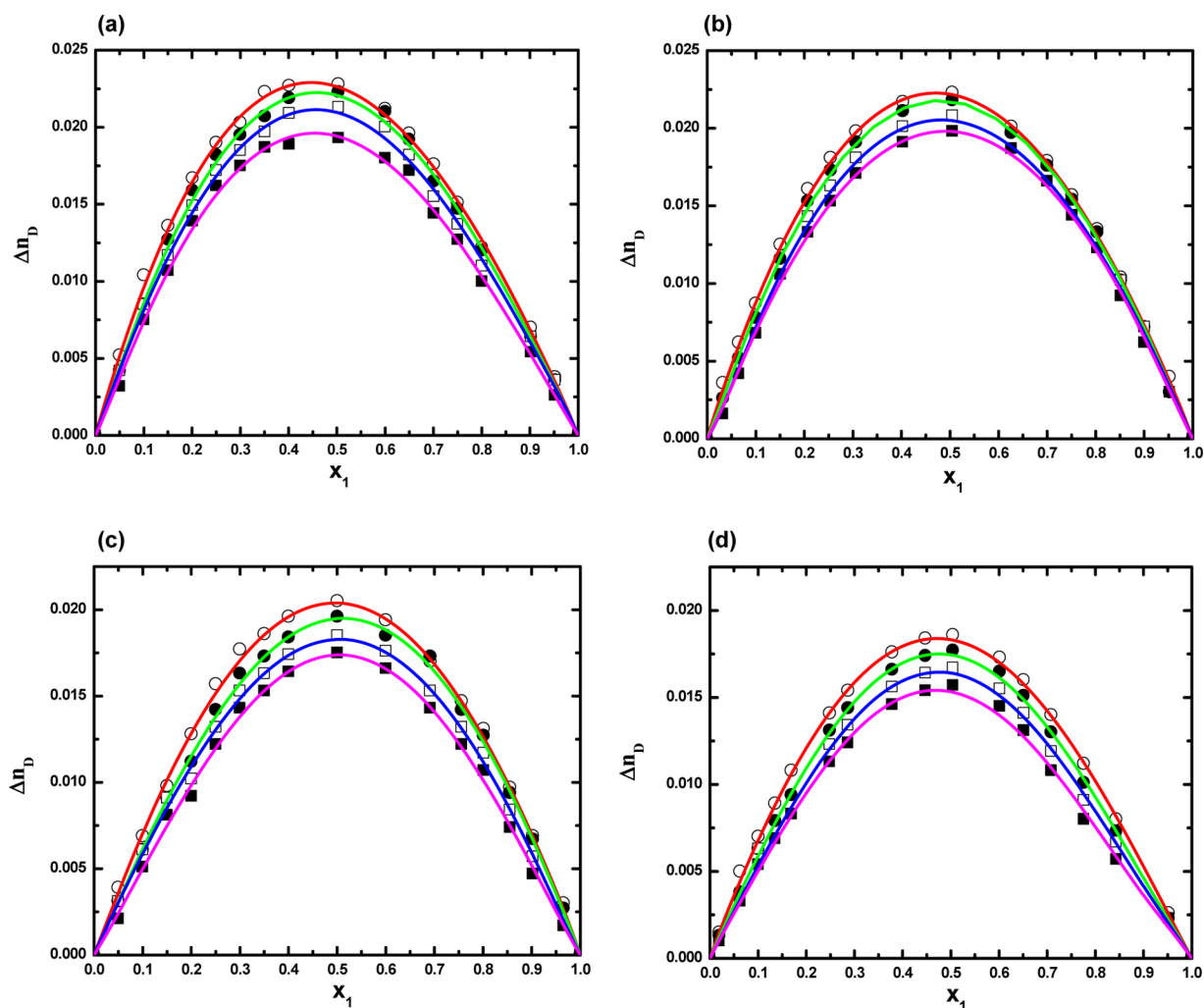


**Figure 12.** Deviation in refractive indices ( $\Delta n_D$ ) for the mixtures of ILs with water as a function of mole fraction ( $x_1$ ) of IL for (a) [TMAH] + water, (b) [TEAH] + water, (c) [TPAH] + water, and (d) [TBAH] + water ( $x_2$ ) at 25 °C (○), 30 °C (●), 35 °C (□), and 40 °C (■). Redlich–Kister correlations are plotted as solid lines.

methyl cation ILs with water are stronger than in the higher alkyl cation chain ILs.

Explicitly, the curves in Figure 11 reveal that the  $\Delta\eta$  values for ammonium-based ILs and water are positive. The positive  $\Delta\eta$  values increase for all ILs with water as the temperature increases, which can be attributed to the hydrogen bonding between water molecules and ILs. When the temperature increases, the interactions become acutely reduced because of the dissociation of ions of the ILs. From these results, the  $\Delta\eta$  values slightly decrease with increasing the alkyl chain length in the cations of ILs, which leads to the decreasing in the interactions from methyl to butyl in the ammonium-based ILs with water.

The temperature dependence of  $\Delta n_D$  of water with ILs displayed in Figure 12. The obtained  $\Delta n_D$  values for ammonium-based ILs with water are positive in the entire composition range of ILs. The maximum is reached around  $x_1 \approx 0.5000$  of IL at all studied temperatures. The positive  $\Delta n_D$  values decrease with increasing alkyl chain length of the cation of ammonium-based ILs. On the other hand, the negative  $V^E$  values also decrease with increasing alkyl chain length in cation of ILs. This is mainly due to less free volume available than in an ideal solution, as can be seen in Figures 5 and 12, which indicate a strong correlation between  $V^E$  and  $\Delta n_D$  quantities for

all the studied systems. We observed negative  $V^E$  values corresponding to positive  $\Delta n_D$  values; the minimum or maximum of both values exist at almost the same mole fraction of IL. Overall, our experimental results explicitly elucidate that there is hydrogen bonding between ions of ILs and water molecules.

## 5. CONCLUSIONS

A combined experimental and COSMO-RS study was used to investigate the molecular interactions between ammonium-based ILs with water at various temperatures. We have estimated  $V^E$ ,  $\Delta\kappa_s$ ,  $\Delta\eta$ , and  $\Delta n_D$  at each temperature as a function of IL concentration and correlated these data with Redlich–Kister type polynomial equations. We have observed negative  $V^E$  and  $\Delta\kappa_s$  values but positive  $\Delta\eta$  and  $\Delta n_D$  values for all ammonium-based ILs with water. This behavior can be explained in terms of hydrogen bonding that is certainly more temperature-dependent. The observed values reveal a more efficient packing or attractive interaction between the IL and water. The prediction based on the COSMO-RS method agrees with the experimental results and significantly indicates that hydrogen bonding is the dominant interaction in the studied

binary system. The observed attractive interactions decrease as alkyl chain lengths of the cations of ILs increase.

## ■ ASSOCIATED CONTENT

### ■ Supporting Information

The Supporting Information is available free of charge on the ACS Publications website at DOI: 10.1021/acs.iecr.5b01796.

Thermophysical properties of ammonium-based ILs with water at various temperatures; activity coefficient of water, specific contributions of enthalpy, and excess enthalpy predicted by COSMO-RS (PDF)

## ■ AUTHOR INFORMATION

### Corresponding Author

\*E-mail: [venkatesup@hotmail.com](mailto:venkatesup@hotmail.com); [pvenkatesu@chemistry.du.ac.in](mailto:pvenkatesu@chemistry.du.ac.in). Tel.: +91-11-27666646-142. Fax: +91-11-2766 6605.

### Notes

The authors declare no competing financial interest.

## ■ ACKNOWLEDGMENTS

We acknowledge the financial support from University of Delhi (R & D Grant RC/2014/6820) and DU-DST Purse Grant (Grant CD/2015/1534). This work was partly developed in the scope of the projects CICECO-Aveiro Institute of Materials (Ref. FCT UID/CTM/S0011/2013) and EXPL/QEQ-PRS/0224/2013 financed by national funds through the FCT/MEC and when applicable cofinanced by FEDER under the PT2020 Partnership Agreement. I.K. also acknowledges Fundação para a Ciência e Tecnologia for the postdoctoral grant SFRH/BPD/76850/2011.

## ■ REFERENCES

- (1) Bosmann, A.; Datsevich, L.; Jess, A.; Lauter, A.; Schmitz, C.; Wasserscheid, P. Deep Desulfurization of Diesel fuel by Extraction with Ionic Liquids. *Chem. Commun.* **2001**, 2494–2495.
- (2) Plechkova, N. V.; Seddon, K. R. Applications of Ionic Liquids in the Chemical Industry. *Chem. Soc. Rev.* **2008**, *37*, 123–150.
- (3) Earle, M. J.; Esperança, J. M. S. S.; Gilea, M. A.; Lopes, J. N. C.; Rebelo, L. P. N.; Magee, J. W.; Seddon, K. R.; Widegren, J. A. The Distillation and Volatility of Ionic Liquids. *Nature* **2006**, *439*, 831–834.
- (4) Kumar, A.; Venkatesu, P. Overview of the Stability of  $\alpha$ -Chymotrypsin in Different Solvent Media. *Chem. Rev.* **2012**, *112*, 4283–4307.
- (5) Attri, P.; Venkatesu, P. Thermodynamic Characterization of the Biocompatible Ionic Liquid Effects on Protein Model Compounds and Their Functional Groups. *Phys. Chem. Chem. Phys.* **2011**, *13*, 6566–6575.
- (6) Hou, M.; Xu, Y.; Han, Y.; Chen, B.; Zhang, W.; Ye, Q.; Sun, J. Thermodynamic Properties of Aqueous Solutions of Two Ammonium-based Protic Ionic Liquids at 298.15 K. *J. Mol. Liq.* **2013**, *178*, 149–155.
- (7) Reddy, P. M.; Umapathi, R.; Venkatesu, P. A Green Approach to offset the Perturbation action of 1-butyl-3-methylimidazolium iodide on  $\alpha$ -Chymotrypsin. *Phys. Chem. Chem. Phys.* **2015**, *17*, 184–190.
- (8) Anouti, M.; Jacquemin, J.; Lemordant, D. Transport properties of protic ionic liquids, pure and in aqueous solutions: Effects of the anion and cation structure. *Fluid Phase Equilib.* **2010**, *297*, 13–22.
- (9) Brunetti, A.; Scura, F.; Barbieri, G.; Drioli, E. Membrane Technologies for CO<sub>2</sub> Separation. *J. Membr. Sci.* **2010**, *359*, 115–125.
- (10) Tiwari, S.; Kumar, A. Diels-Alder Reactions Are Faster in Water than in Ionic Liquids at Room Temperature. *Angew. Chem.* **2006**, *118*, 4942–4943.
- (11) Ventura, S. P. M.; Marques, C. S.; Rosatella, A. A.; Afonso, C. A. M.; Goncalves, F.; Coutinho, J. A. P. Toxicity assessment of various

ionic liquid families towards *Vibrio fischeri* marine bacteria. *Ecotoxicol. Environ. Saf.* **2012**, *76*, 162–168.

(12) Blanchard, L. A.; Gu, Z.; Brennecke, J. F. High-Pressure Phase Behavior of Ionic Liquid/CO<sub>2</sub> Systems. *J. Phys. Chem. B* **2001**, *105*, 2437–2444.

(13) Anderson, J. L.; Armstrong, D. W. High-Stability Ionic Liquids. A New Class of Stationary Phases for Gas Chromatography. *Anal. Chem.* **2003**, *75*, 4851–4858.

(14) Nguyen, N. L.; Rochefort, D. Electrochemistry of Ruthenium Dioxide Composite Electrodes in Diethylmethylammonium-triflate Protic Ionic Liquid and Its Mixtures with Acetonitrile. *Electrochim. Acta* **2014**, *147*, 96–103.

(15) Sun, X.; Do-Thanh, C. L.; Luo, H.; Dai, S. The Optimization of an Ionic Liquid-Based TALSPEAK-like Process for Rare Earth Ions Separation. *Chem. Eng. J.* **2014**, *239*, 392–398.

(16) Qiu, B.; Lin, B.; Qiu, L.; Yan, F. Alkaline Imidazolium- and Quaternary Ammonium-Functionalized Anion Exchange Membranes for Alkaline Fuel Cell Applications. *J. Mater. Chem.* **2012**, *22*, 1040–1045.

(17) Smith, A. M.; Parkes, M. A.; Perkin, S. Molecular Friction Mechanisms Across Nanofilms of a Bilayer-Forming Ionic Liquid. *J. Phys. Chem. Lett.* **2014**, *5*, 4032–4037.

(18) Jha, I.; Attri, P.; Venkatesu, P. Unexpected Effects of the Alteration of Structure and Stability of Myoglobin and Hemoglobin in Ammonium-Based Ionic Liquids. *Phys. Chem. Chem. Phys.* **2014**, *16*, 5514–5526.

(19) Attri, P.; Venkatesu, P.; Kumar, A. Activity and Stability of  $\alpha$ -Chymotrypsin in Biocompatible Ionic Liquids: Enzyme Refolding by Triethylammonium acetate. *Phys. Chem. Chem. Phys.* **2011**, *13*, 2788–2796.

(20) Binetti, E.; Panniello, A.; Triggiani, L.; Tommasi, R.; Agostiano, A.; Curri, M. L.; Striccoli, M. Spectroscopic Study on Imidazolium-Based Ionic Liquids: Effect of Alkyl Chain Length and Anion. *J. Phys. Chem. B* **2012**, *116*, 3512–3518.

(21) Khan, I.; Kurnia, K. A.; Mutelet, F.; Pinho, S. P.; Coutinho, J. A. Probing the Interactions Between Ionic Liquids And Water: Experimental and Quantum Chemical Approach. *J. Phys. Chem. B* **2014**, *118*, 1848–1860.

(22) Gonzalez-Miquel, M.; Bedia, J.; Abrusci, C.; Palomar, J.; Rodriguez, F. Anion Effects on Kinetics and Thermodynamics of CO<sub>2</sub> Absorption in Ionic Liquids. *J. Phys. Chem. B* **2013**, *117*, 3398–3406.

(23) Kurnia, K. A.; Pinho, S. P.; Coutinho, J. A. P. Designing Ionic Liquids for Absorptive Cooling. *Green Chem.* **2014**, *16*, 3741–3745.

(24) Migliorati, V.; Zitolo, A.; D'Angelo, P. Using a Combined Theoretical and Experimental Approach to Understand the Structure and Dynamics of Imidazolium-Based Ionic Liquids/Water Mixtures. I. MD Simulations. *J. Phys. Chem. B* **2013**, *117*, 12505–12515.

(25) Shi, W.; Myers, C. R.; Luebke, D. R.; Steckel, J. A.; Sorescu, D. C. Theoretical and Experimental Studies of CO<sub>2</sub> and H<sub>2</sub> Separation Using the 1-Ethyl-3-Methylimidazolium Acetate ([emim][CH<sub>3</sub>COO]) Ionic Liquid. *J. Phys. Chem. B* **2012**, *116*, 283–295.

(26) Swatloski, R. P.; Spear, S. K.; Holbrey, J. D.; Rogers, R. D. Dissolution of Cellulose with Ionic Liquids. *J. Am. Chem. Soc.* **2002**, *124*, 4974–4975.

(27) Goodrich, B. F.; de la Fuente, J. C.; Gurkan, B. E.; Lopez, Z. K.; Price, E. A.; Huang, Y.; Brennecke, J. F. Effect of Water and Temperature on Absorption of CO<sub>2</sub> by Amine-functionalized Anion-tethered Ionic Liquids. *J. Phys. Chem. B* **2011**, *115*, 9140–9150.

(28) Zheng, D.; Dong, L.; Huang, W.; Wu, X.; Nie, N. A Review of Imidazolium Ionic Liquids Research and Development towards Working Pair of Absorption Cycle. *Renewable Sustainable Energy Rev.* **2014**, *37*, 47–68.

(29) Passos, H.; Khan, I.; Mutelet, F.; Oliveira, M. B.; Carvalho, P. J.; Santos, L. M. N. B. F.; Held, C.; Sadowski, G.; Freire, M. G.; Coutinho, J. A. P. Vapor-Liquid Equilibria of Water plus Alkylimidazolium-based Ionic Liquids: Measurements and Perturbed-Chain Statistical Associating Fluid Theory Modeling. *Ind. Eng. Chem. Res.* **2014**, *53*, 3737–3748.

- (30) Khamooshi, M.; Parham, K.; Atikol, U. Overview of Ionic Liquids used as Working Fluids in Absorption Cycles. *Adv. Mech. Eng.* **2013**, *2013*, 1–7.
- (31) Khan, I.; Kurnia, K. A.; Sintra, T. E.; Saraiva, J. A.; Pinho, S. P.; Coutinho, J. A. P. Assessing the Activity Coefficients of Water in Cholinium-based Ionic Liquids: Experimental Measurements and COSMO-RS Modeling. *Fluid Phase Equilib.* **2014**, *361*, 16–22.
- (32) Carvalho, P. J.; Khan, I.; Morais, A.; Granjo, J. F. O.; Oliveira, N. M. C.; Santos, L. M. N. B. F.; Coutinho, J. A. P. A New Microbullimeter for the Measurement of the Vapor-Liquid Equilibrium of Ionic Liquid Systems. *Fluid Phase Equilib.* **2013**, *354*, 156–165.
- (33) Freire, M. G.; Claudio, A. F. M.; Araujo, J. M. M.; Coutinho, J. A. P.; Marrucho, I. M.; Lopes, J. N. C.; Rebelo, L. P. N. Aqueous Biphasic Systems: a Boost Brought About by Using Ionic Liquids. *Chem. Soc. Rev.* **2012**, *41*, 4966–4995.
- (34) Umapathi, R.; Attri, P.; Venkatesu, P. Thermophysical Properties of Aqueous Solution of Ammonium-Based Ionic Liquids. *J. Phys. Chem. B* **2014**, *118*, 5971–5982.
- (35) Khan, I.; Taha, M.; Ribeiro-Claro, P.; Pinho, S. P.; Coutinho, J. A. P. Effect of the Cation on the Interactions between Alkyl Methyl Imidazolium Chloride Ionic Liquids and Water. *J. Phys. Chem. B* **2014**, *118*, 10503–10514.
- (36) Terranova, Z. L.; Corcelli, S. A. Molecular Dynamics Investigation of the Vibrational Spectroscopy of Isolated Water in an Ionic Liquid. *J. Phys. Chem. B* **2014**, *118*, 8264–8272.
- (37) Bahadur, I.; Letcher, T. M.; Singh, S.; Redhi, G. G.; Venkatesu, P.; Ramjugernath, D. Excess Molar Volumes of Binary Mixtures (an ionic liquid + water): A review. *J. Chem. Thermodyn.* **2015**, *82*, 34–46.
- (38) Gómez, E.; González, B.; Calvar, N.; Domínguez, A. Excess Molar Properties of Ternary System (Ethanol + Water + 1,3-Dimethylimidazolium Methylsulphate) and Its Binary Mixtures at Several temperatures. *J. Chem. Thermodyn.* **2008**, *40*, 1208–1216.
- (39) Zhang, S.; Li, X.; Chen, H.; Wang, J.; Zhang, J.; Zhang, M. Determination of Physical Properties for the Binary System of 1-ethyl-3-methylimidazolium Tetrafluoroborate + H<sub>2</sub>O. *J. Chem. Eng. Data* **2004**, *49*, 760–764.
- (40) Domańska, U.; Królikowska, M.; Królikowski, M. Phase Behaviour and Physico-Chemical Properties of the Binary Systems {1-Ethyl-3-methylimidazolium Thiocyanate, or 1-Ethyl-3-methylimidazolium Tosylate + Water, or + Alcohols}. *Fluid Phase Equilib.* **2010**, *294*, 72–83.
- (41) García-Miaja, G.; Troncoso, J.; Romani, L. Excess Enthalpy, Density, and Heat Capacity for Binary Systems of Alkylimidazolium-Based Ionic Liquids + Water. *J. Chem. Thermodyn.* **2009**, *41*, 161–166.
- (42) Gómez, E.; González, B.; Calvar, N.; Tojo, E.; Domínguez, A. Physical Properties of Pure 1-Ethyl-3-methylimidazolium Ethylsulfate and Its Binary Mixtures with Ethanol and Water at Several Temperatures. *J. Chem. Eng. Data* **2006**, *51*, 2096–2102.
- (43) Lehmann, J.; Rausch, M. H.; Leipertz, A.; Fröba, A. P. Densities and Excess Molar Volumes for Binary Mixtures of Ionic Liquid 1-Ethyl-3-methylimidazolium Ethylsulfate with Solvents. *J. Chem. Eng. Data* **2010**, *55*, 4068–4074.
- (44) Bhattacharjee, A.; Varanda, C.; Freire, M. G.; Matted, S.; Santos, L. M. N. B. F.; Marrucho, I. M.; Coutinho, J. A. P. Density and Viscosity Data for Binary Mixtures of 1-Alkyl-3-methylimidazolium Alkylsulfates + Water. *J. Chem. Eng. Data* **2012**, *57*, 3473–3482.
- (45) Navarro, P.; Larriba, M.; García, S.; García, J.; Rodríguez, F. Physical Properties of Binary and Ternary Mixtures of 2-Propanol, Water, and 1-Butyl-3-methylimidazolium Tetrafluoroborate Ionic Liquid. *J. Chem. Eng. Data* **2012**, *57*, 1165–1173.
- (46) Vercher, E.; Miguel, P. J.; Llopis, F. J.; Orchilles, A. V.; Martínez-Andreu, A. Volumetric and Acoustic Properties of Aqueous Solutions of Trifluoromethanesulfonate-Based Ionic Liquids at Several Temperatures. *J. Chem. Eng. Data* **2012**, *57*, 1953–1963.
- (47) Gonzalez, E. J.; Domínguez, A.; Macedo, E. A. Physical and Excess Properties of Eight Binary Mixtures Containing Water and Ionic Liquids. *J. Chem. Eng. Data* **2012**, *57*, 2165–2176.
- (48) Sastry, N. V.; Vaghela, N. M.; Macwan, P. M. Densities, Excess Molar and Partial Molar Volumes for Water+ 1-Butyl- or, 1-Hexyl- or, 1-Octyl-3-methylimidazolium Halide Room Temperature Ionic Liquids at T= (298.15 and 308.15) K. *J. Mol. Liq.* **2013**, *180*, 12–18.
- (49) Ficke, L. E.; Novak, R. R.; Brennecke, J. F. Thermodynamic and Thermophysical Properties of Ionic Liquid + Water Systems. *J. Chem. Eng. Data* **2010**, *55*, 4946–4950.
- (50) Golzar, K.; Amjad-Iranagh, S.; Modarress, H. Prediction of Thermophysical Properties for Binary Mixtures of Common Ionic Liquids with Water or Alcohol at Several Temperatures and Atmospheric Pressure by Means of Artificial Neural Network. *Ind. Eng. Chem. Res.* **2014**, *53*, 7247–7262.
- (51) Chen, J.; Chen, L.; Lu, Y.; Xu, Y. Physicochemical Properties of Aqueous Solution of 1-Methylimidazolium Acetate Ionic Liquid at Several Temperatures. *J. Mol. Liq.* **2014**, *197*, 374–380.
- (52) Mokhtarani, B.; Sharifi, A.; Mortaheb, H. R.; Mirzaei, M.; Mafi, M.; Sadeghian, F. Density and Viscosity of Pyridinium-Based Ionic Liquids and Their Binary Mixtures with Water at Several Temperatures. *J. Chem. Thermodyn.* **2009**, *41*, 323–329.
- (53) García-Miaja, G.; Troncoso, J.; Romani, L. Density and Heat Capacity as a Function of Temperature for Binary Mixtures of 1-Butyl-3-methylpyridinium Tetrafluoroborate + Water, + Ethanol, and + Nitromethane. *J. Chem. Eng. Data* **2007**, *52*, 2261–2265.
- (54) Wang, J. Y.; Zhang, X. J.; Hu, Y. Q.; Qi, G. D.; Liang, L. Y. Properties of n-Butylpyridinium Nitrate Ionic Liquid and Its Binary Mixtures with Water. *J. Chem. Thermodyn.* **2012**, *45*, 43–47.
- (55) Neves, C. M. S. S.; Batista, M. L. S.; Cláudio, A. F. M.; Santos, L. M. N. B. F.; Marrucho, I. M.; Freire, M. G.; Coutinho, J. A. P. Thermophysical Properties and Water Saturation of [PF<sub>6</sub>]-Based Ionic Liquids. *J. Chem. Eng. Data* **2010**, *55*, 5065–5073.
- (56) Domańska, U.; Królikowska, M. Density and Viscosity of Binary Mixtures of Thiocyanate Ionic Liquids + Water as a Function of Temperature. *J. Solution Chem.* **2012**, *41*, 1422–1445.
- (57) Królikowska, M.; Zawadzki, M.; Królikowski, M. Physicochemical and Thermodynamic Study on Aqueous Solutions of Dicyanamide-Based Ionic Liquids. *J. Chem. Thermodyn.* **2014**, *70*, 127–137.
- (58) Królikowska, M.; Lipinski, P.; Maik, D. Density, Viscosity and Phase Equilibria Study of {Ethylsulfate-Based Ionic Liquid + Water} Binary Systems as a Function of Temperature and composition. *Thermochim. Acta* **2014**, *582*, 1–9.
- (59) Anouti, M.; Vigeant, A.; Jacquemin, J.; Brigouleix, C.; Lemordant, D. Volumetric Properties, Viscosity and Refractive Index of the Protic Ionic Liquid, Pyrrolidinium Octanoate, in Molecular Solvents. *J. Chem. Thermodyn.* **2010**, *42*, 834–845.
- (60) Zawadzki, M.; Królikowska, M.; Lipinski, P. Physicochemical and Thermodynamic Characterization of N-alkyl-Nmethylpyrrolidinium Bromides and Its Aqueous Solutions. *Thermochim. Acta* **2014**, *589*, 148–157.
- (61) Blahušiak, M.; Schlosser, Š. Physical properties of Phosphonium Ionic Liquid and Its Mixtures with Dodecane and Water. *J. Chem. Thermodyn.* **2014**, *72*, 54–64.
- (62) Neves, C. M. S. S.; Carvalho, P. J.; Freire, M. G.; Coutinho, J. A. P. Thermophysical Properties of Pure and Water-Saturated Tetradecyltrihexylphosphonium-Based Ionic Liquids. *J. Chem. Thermodyn.* **2011**, *43*, 948–957.
- (63) Zarrougui, R.; Dhahbi, M.; Lemordant, D. Transport and Thermodynamic Properties of Ethylammonium Nitrate–Water Binary Mixtures: Effect of Temperature and Composition. *J. Solution Chem.* **2015**, *44*, 686.
- (64) Alvarez, V. H.; Mattedi, S.; Martin-Pastor, M.; Aznar, M.; Iglesias, M. Thermophysical Properties of Binary Mixtures of {Ionic Liquid 2-Hydroxyethylammonium Acetate + (Water, Methanol, or Ethanol)}. *J. Chem. Thermodyn.* **2011**, *43*, 997–1010.
- (65) Hou, M.; Xu, Y.; Han, Y.; Chen, B.; Zhang, W.; Ye, Q.; Sun, J. Thermodynamic Properties of Aqueous Solutions of Two Ammonium-Based Protic Ionic Liquids at 298.15 K. *J. Mol. Liq.* **2013**, *178*, 149–155.
- (66) Xu, Y. Volumetric, Viscosity, and Electrical Conductivity Properties of Aqueous Solutions of Two n-Butylammonium-Based

Protic Ionic Liquids at Several Temperatures. *J. Chem. Thermodyn.* **2013**, *64*, 126–133.

(67) Taib, M. M.; Murugesan, T. Densities and Excess Molar Volumes of Binary Mixtures of Bis(2-hydroxyethyl)ammonium Acetate + Water and Monoethanolamine + Bis(2-hydroxyethyl)ammonium Acetate at Temperatures from (303.15 to 353.15) K. *J. Chem. Eng. Data* **2010**, *55*, 5910–5913.

(68) Arce, A.; Soto, A.; Ortega, J.; Sabater, G. Viscosities and Volumetric Properties of Binary and Ternary Mixtures of Tris(2-hydroxyethyl) Methylammonium Methylsulfate + Water + Ethanol at 298.15 K. *J. Chem. Eng. Data* **2008**, *53*, 770–775.

(69) Kumar, A.; Venkatesu, P. Prevention of Insulin Self-aggregation by a Protic Ionic Liquid. *RSC Adv.* **2013**, *3*, 362–367.

(70) Kavitha, T.; Attri, P.; Venkatesu, P.; Rama Devi, R. S.; Hofman, T. Influence of Alkyl Chain Length and Temperature on Thermophysical Properties of Ammonium-Based Ionic Liquids with Molecular Solvent. *J. Phys. Chem. B* **2012**, *116*, 4561–4574.

(71) Govinda, V.; Attri, P.; Venkatesu, P.; Venkateswarlu, P. Evaluation of Thermophysical Properties of Ionic Liquids with Polar Solvent: A Comparable Study of Two Families of Ionic Liquids with Various Ions. *J. Phys. Chem. B* **2013**, *117*, 12535–12548.

(72) Attri, P.; Venkatesu, P.; Kumar, A. Temperature Effect on the Molecular Interactions between Ammonium Ionic Liquids and N,N-Dimethylformamide. *J. Phys. Chem. B* **2010**, *114*, 13415–13425.

(73) Hizaddin, H. F.; Hashim, M. A.; Anantharaj, R. Evaluation of Molecular Interaction in Binary Mixture of Ionic Liquids + Heterocyclic Nitrogen Compounds: Ab Initio Method and COS-MORS Model. *Ind. Eng. Chem. Res.* **2013**, *52*, 18043–18058.

(74) Klamt, A. *COSMO-RS from Quantum Chemistry to Fluid Phase Thermodynamics and Drug Design*; Elsevier: Amsterdam, The Netherlands, 2005.

(75) Kurnia, K. A.; Coutinho, J. A. P. Overview of the Excess Enthalpies of the Binary Mixtures Composed of Molecular Solvents and Ionic Liquids and their Modeling Using COSMO-RS. *Ind. Eng. Chem. Res.* **2013**, *52*, 13862–13874.

(76) Klamt, A.; Schüürmann, G. COSMO: A New Approach to Dielectric Screening in Solvents with Explicit Expressions for the Screening Energy and its Gradient. *J. Chem. Soc., Perkin Trans. 2* **1993**, *2*, 799–805.

(77) Klamt, A. *From Quantum Chemistry to Fluid Phase Thermodynamics and Drug Design*. Elsevier: Amsterdam, 2005; pp. 1–217.

(78) Diedenhofen, M.; Eckert, F.; Klamt, A. Prediction of Infinite Dilution Activity Coefficients of Organic Compounds in Ionic Liquids using COSMO-RS. *J. Chem. Eng. Data* **2003**, *48*, 475–479.

(79) Putnam, R.; Taylor, R.; Klamt, A.; Eckert, F.; Schiller, M. Prediction of Infinite Dilution Activity Coefficients using COSMO-RS. *Ind. Eng. Chem. Res.* **2003**, *42*, 3635–3641.

(80) Zorębski, E.; Geppert-Rybczynska, M.; Zorębski, M. Acoustics as a Tool for Better Characterization of Ionic Liquids: A Comparative Study of 1-Alkyl-3-methylimidazolium bis[(trifluoromethyl)sulfonyl]imide Room-temperature Ionic Liquids. *J. Phys. Chem. B* **2013**, *117*, 3867–3876.

(81) Cammarata, L.; Kazarian, S. G.; Salter, P. A.; Welton, T. Molecular States of Water in Room Temperature Ionic Liquids. *Phys. Chem. Chem. Phys.* **2001**, *3*, 5192–5200.

(82) Moreno, M.; Castiglione, F.; Mele, A.; Pasqui, C.; Raos, G. Interaction of Water with the Model Ionic Liquid [bmim][BF<sub>4</sub>]: Molecular Dynamics Simulations and Comparison with NMR Data. *J. Phys. Chem. B* **2008**, *112*, 7826–7836.

(83) Zhang, Q.-G.; Wang, N.-N.; Yu, Z.-W. The Hydrogen Bonding Interactions between the Ionic Liquid 1-Ethyl-3-methylimidazolium Ethylsulfate and Water. *J. Phys. Chem. B* **2010**, *114*, 4747–4754.

(84) Singh, T.; Kumar, A. Cation-Anion-Water Interactions in Aqueous Mixtures of Imidazolium based Ionic Liquids. *Vib. Spectrosc.* **2011**, *55*, 119–125.

(85) Freire, M. G.; Santos, L. M. N. B. F.; Fernandes, A. M.; Coutinho, J. A. P.; Marrucho, I. M. An Overview of the Mutual

Solubilities of Water-Imidazolium-based Ionic Liquids Systems. *Fluid Phase Equilib.* **2007**, *261*, 449–454.

(86) García-Miaja, G.; Troncoso, J.; Román, L. Excess Enthalpy, Density, and Heat Capacity for Binary Systems of Alkylimidazolium-based Ionic Liquids + Water. *J. Chem. Thermodyn.* **2009**, *41*, 161–166.